ing IL-2 and chemokine. Supernatants were harvested on day 9 and assayed for p24 levels.On U87/CD4 cells, virus infectivity was assessed by a focus-forming assay as described [G. Simmons *et al.*, *Science* **276,** 276 (1997)]. Briefly, for viruses using more than one coreceptor, focus-forming units (FFUs) were assessed separately for each appropriate coreceptor expressing U87/CD4 cell type. Cells were seeded into 48-well trays at 1 × 10^4 cells per well overnight. The cells were then treated for 30 min at 37°C with appropriate concentrations of chemokine in 75 μl. One hundred FFUs of each virus in 75 μl were added and incubated for 3 hours at 37°C. The cells were then washed three times, and 500 μl of medium containing the appropriate chemokine at the correct concentration was added. After 5 days the cells were fixed for 10 min in cold acetone:methanol (1:1) and immunostained for in situ p24 as described [Á. McKnight, P. R. Clapham, R. A. Weiss, *Virology* **201**, 8 (1994)]. Standard errors were estimated from duplicate wells, and the results (Fig. 1) are representative of three separate experiments.
16. M. J. Endres *et al.*, *Cell* **87**, 745 (1996); J. D. Reeves *et al.*, *Virology* **231**, 130 (1997).
17. Neither RANTES, vMIP-I, nor vMIP-II had appreciable effect on SF162 infection of U87/CD4 CCR5 cells, whereas vMIP-II and vMIP-I blocked infection by SL-2 at 400 nM by more than 50 and 25%, respectively. vMIP-II, but not vMIP-I, blocked the SI strains 89.6 and 2028 at 200 nM by 50 and 20%, respectively, compared with RANTES, which blocked infection of these viruses completely at 100 nM. On U87/CD4 CXCR4 cells, both vMIP-I and vMIP-II showed little activity (10 to 30% inhibition at 200 nM) in blocking infection by strain 89.6 or 2028. On U87 CXCR4 cells (CD4 negative), inhibition of infection by HIV-2 ROD/B was ~50% at 200 nM by vMIP-I and vMIP-II.
18. P. D. Ponath *et al.*, *J. Exp. Med.* **183**, 2437 (1996); B. L. Daugherty *et al.*, *ibid.*, p. 2349.
19. Human eosinophils and neutrophils were isolated from the peripheral blood of healthy volunteers as described [P. J. Jose *et al.*, *J. Exp. Med.* **179**, 881 (1994)]. Briefly, neutrophils (>95% purity, contaminating cells being a mixture of eosinophils and mononuclear cells) were separated from red blood cells and mononuclear cells by sequential dextran sedimentation and Percoll–plasma density centrifugation. Eosinophils (>98% purity, contaminating cells being mononuclear cells) were isolated from healthy atopic individuals as described above for neutrophils followed by immunomagnetic separation of the eosinophils from the neutrophils with anti-CD16 microbeads as described (*32*). Calcium mobilization in purified neutrophils and eosinophils was measured as described (*32*). Briefly, purified neutrophils or eosinophils were incubated with fura-2 acetoxy-methyl ester (1 to 2.5 μM), washed three times in 10 mM PBS (without Ca^{2+} or Mg^{2+}) + 0.1% bovine serum albumin (BSA) (200*g*, 8 min), and resuspended at 2 × 10^6 cells/ml in 10 mM PBS (without Ca^{2+} or Mg^{2+}) + 0.25% BSA + 10 mM Hepes + 10 mM glucose. Aliquots of cells were placed in quartz cuvettes, and the external Ca^{2+} concentration was adjusted to 1 mM with $CaCl_2$. Changes in fluorescence were measured at 37°C by means of a fluorescence spectrophotometer at excitation wavelengths of 340 and 380 nm and an emission wavelength 510 nm. Intracellular Ca^{2+} concentration $[Ca^{2+}]_i$ was calculated with the ratio of the two fluorescence readings and a dissociation constant for Ca^{2+} at 37°C of 224 nM. In experiments designed to investigate desensitization between agonists, the first agonist (the desensitizing agonist) was added after 50 s and the second agonist added 150 s later.
20. A. E. I. Proudfoot *et al.*, *J. Biol. Chem.* **271**, 2599 (1996); B. Moser *et al.*, *ibid.* **268**, 7125 (1993).
21. K. Neote, D. DiGregorio, J. Y. Mak, R. Horuk, T. J. Schall, *Cell* **72**, 415 (1993); J. L. Gao *et al.*, *J. Exp. Med.* **177**, 1421 (1993).
22. Human eosinophils (5 × 10^5 cells/100 μl per well) were placed in 3-μm pore size transwell inserts and placed in cell culture wells containing 400 μl of human eotaxin, vMIP-I, or vMIP-II at various concentrations of buffer [RPMI 1640 + L-glutamine + 2% fetal calf serum + 10 mM Hepes (pH 7.4)] as described [P. D. Ponath *et al.*, *J. Exp. Med.* **183**, 2437 (1996)]. After incubation at 37°C for 60 min (95% O_2, 5% CO_2), eosinophils migrating through the transwell were counted on a FACScan flow cytometer (Becton Dickinson).
23. W. Risau, *Nature* **387**, 671 (1997).
24. A. L. Angiolillo, C. Sgadari, G. Tosato, *Ann. N.Y. Acad. Sci.* **795**, 158 (1996); R. M. Strieter *et al.*, *J. Biol. Chem.* **270**, 27348 (1995); Y. Cao, C. Chen, J. A. Weatherbee, M. Tsang, J. Folkman, *J. Exp. Med.* **182**, 2069 (1995).
25. D. Knighton, D. Ausprunk, D. Tapper, J. Folkman, *Br. J. Cancer* **35**, 347 (1977); P. C. Brooks, R. A. F. Clark, D. A. Cheresh, *Science* **264**, 569 (1994); M. Friedlander *et al.*, *ibid.* **270**, 1500 (1995).
26. Angiogenic activities of synthetically prepared viral and human chemokines were evaluated by the chick CAM assay as described [T. Oikawa *et al.*, *Cancer Lett.* **59**, 57 (1991)]. Fertilized Plymouth Rock × White Leghorn eggs were incubated at 37°C in a humidified atmosphere (relative humidity, ~70%). Test samples were dissolved in sterile distilled water or PBS. Sterilized sample solution was mixed with an equal volume of autoclaved 2% methylcellulose. Controls were prepared with vehicle only (1% methylcellulose solution). The sample solution (20 μl) was dropped on Parafilm and dried up. The methylcellulose disks were stripped off from the Parafilm and placed on a CAM of 10- or 11-day-old chick embryos. After 3 days, the CAMs were observed by means of an Olympus stereoscope. A 20% fat emulsion (Intralipos 20%, Midori-Juji, Osaka, Japan) was injected into the CAM to increase the contrast between blood and surrounding tissues [R. Danesi *et al.*, *Clin. Cancer Res.* **3**, 265 (1997)]. The CAMs were photographed for evaluation of angiogenic response. Angiogenic responses were graded independently by three investigators as negative, positive, or unclear on the basis of infiltration of blood vessels into the area of the implanted methylcellulose.
27. T. Kledal *et al.*, *Science* **277**, 1656 (1997).
28. J. He *et al.*, *Nature* **385**, 645 (1997).
29. S. A. Miles *et al.*, *Proc. Natl. Acad. Sci. U.S.A.* **87**, 4068 (1990); K. Yoshizaki *et al.*, *Blood* **74**, 1360 (1989); K. Weindel, D. Marme, H. A. Weich, *Biochem. Biophys. Res. Commun.* **183,** 1167(1992); R. Masood *et al.*, *Proc. Natl. Acad. Sci. U.S.A.* **94,** 979 (1997).
30. C. Boshoff *et al.*, unpublished data.
31. G. Simmons *et al.*, *J. Virol.* **70**, 8355 (1996).
32. P. J. Jose *et al.*, *J. Exp. Med.* **179,** 881 (1994).
33. We thank D. Littman and J Hoxie for providing U87/CD4 cells, and P. Clapham and G. Simmons for doing HIV-1 experiments. Supported by the Cancer Research Campaign; the Medical Research Council; the Japanese Ministry of Health and Welfare; the Japanese Ministry of Education, Sciences, Sports and Culture; the Wellcome Trust; The National Asthma Campaign; and NCI (CA 67391).

1 July 1997; accepted 2 September 1997

Caspase-3–Generated Fragment of Gelsolin: Effector of Morphological Change in Apoptosis

Srinivas Kothakota,* Toshifumi Azuma,* Christoph Reinhard, Anke Klippel, Jay Tang, Keting Chu, Thomas J. McGarry, Marc W. Kirschner, Kirston Koths, David J. Kwiatkowski,† Lewis T. Williams

The caspase-3 (CPP32, apopain, YAMA) family of cysteinyl proteases has been implicated as key mediators of apoptosis in mammalian cells. Gelsolin was identified as a substrate for caspase-3 by screening the translation products of small complementary DNA pools for sensitivity to cleavage by caspase-3. Gelsolin was cleaved in vivo in a caspase-dependent manner in cells stimulated by Fas. Caspase-cleaved gelsolin severed actin filaments in vitro in a Ca^{2+}-independent manner. Expression of the gelsolin cleavage product in multiple cell types caused the cells to round up, detach from the plate, and undergo nuclear fragmentation. Neutrophils isolated from mice lacking gelsolin had delayed onset of both blebbing and DNA fragmentation, following apoptosis induction, compared with wild-type neutrophils. Thus, cleaved gelsolin may be one physiological effector of morphologic change during apoptosis.

A conserved family of aspartate-specific cysteinyl proteases (caspases) has been identified as critical mediators of apoptosis in *Caenorhabditis elegans* and mammals (*1*, *2*). Although multiple protein substrates of caspases have been found, the functional significance of the substrates is poorly understood (*3*). We reasoned that an unbiased approach to determine proteins that were the best substrates of caspase-3 in vitro would yield a physiologically relevant substrate. Therefore, we constructed a protein library by translating a murine embryo cDNA library in vitro (*4*) and tested the translated proteins for their sensitivity to caspase-3 cleavage. To facilitate screening, we separated the cDNAs into small pools before in vitro translation and incorporated [^{35}S]methionine into the translation mix to

S. Kothakota, C. Reinhard, A. Klippel, K. Chu, K. Koths, L. T. Williams, Chiron Corporation, Emeryville, CA 94608, USA.
T. Azuma, J. Tang, D. J. Kwiatkowski, Division of Experimental Medicine, Brigham and Women's Hospital, Boston, MA 02115, USA.
T. J. McGarry and M. W. Kirschner, Department of Cell Biology, Harvard Medical School, Boston, MA 02115, USA.

*These authors contributed equally to this work.
†To whom correspondence should be addressed. E-mail: kwiatkowski@calvin.bwh.harvard.edu

label the proteins. The translated pools were separated into two parts; one portion was incubated with active caspase-3, and the other portion was incubated with caspase-3 inactivated by the addition of *N*-acetyl-Asp-Glu-Val-Asp–fluoromethyl ketone (DEVD-fmk) (*2*). The reaction products were resolved by SDS–polyacrylamide gel electrophoresis (PAGE), and protein targets of caspase-3 were identified by comparing the pattern of ^{35}S-labeled proteins in the samples treated with active and inactive caspase-3. To avoid false positives, we found it necessary to carefully titrate the amount of enzyme. We used an amount sufficient to cleave 80% of a known substrate of caspase-3, baculovirus protein p35 (Fig. 1A) (*5*).

One thousand cDNA pools, each containing 100 cDNA clones (100,000 cDNA clones total), were screened to identify substrates of caspase-3. In three different pools, incubation of active caspase-3 with labeled proteins reduced the intensity of a 65-kD band and generated a new band at 48 kD (Fig. 1A, pool 4). To identify the cDNA clone encoding the 65-kD protein, the DNA from the positive pools was used to transform *Escherichia coli*, and the DNA prepared from single colonies was screened again. DNA sequencing and polymerase chain reaction analyses of the single positive clone from all three pools identified the 65-kD protein as the partial sequence of gelsolin from residues 142 to 731.

Caspase-3 rapidly cleaved full-length recombinant murine gelsolin, confirming that gelsolin is a substrate for caspase-3 (Fig. 1B). Gelsolin was also cleaved upon incubation with cell extracts prepared from cells that were induced to undergo apoptosis by Fas activation (*6*). However, no gelsolin cleavage activity was observed in cell extracts prepared from untreated cells. Protein microsequencing by Edman degradation was used to determine the NH_2-terminal sequences of the cleavage products and indicated a cleavage site between residues Asp^{352} and Gly^{353} of murine gelsolin, so that products had actual molecular masses of 39 (NH_2-terminal) and 41 (COOH-terminal) kD. The sequence in this region, Asp^{349}-Gln-Thr-Asp-Gly^{353}, is consistent with the known requirements for efficient cleavage by caspase-3 (*2*) and is conserved between mouse, human, and porcine gelsolin (*7*). Cleavage of gelsolin also resulted in dissociation of the 39- and 41-kD cleavage products when assayed by size-exclusion chromatography (*8*).

To examine cleavage of gelsolin during apoptosis in vivo, initially we used a model cell system in which apoptosis is highly inducible (*9*). The assay used fibroblasts that expressed a chimeric receptor composed of the extracellular and transmembrane domains of murine CD4 and the cytoplasmic domain of Fas. Apoptosis was induced by antibody cross-linking of the extracellular CD4 domains. Gelsolin was cleaved into the predicted 39- and 41-kD products 30 min after apoptosis induction (Fig. 2A). Cleavage of gelsolin occurred early and was comparable to the time course of cleavage of poly–adenosine diphosphate ribose polymerase (PARP), a substrate of caspase-3 (Fig. 2A). Both gelsolin and PARP cleavage was blocked by the cell-permeable inhibitor of caspase-3, *N*-benzyloxycarbonyl-Val-Ala-Asp–fmk (zVAD-fmk) (*10*). Gelsolin cleavage was specific, because another cytoskeletal protein, filamin, was not cleaved under identical conditions (Fig. 2A). Thus, gelsolin was specifically cleaved by a caspase-3–like enzyme in vivo, and this cleavage is an early step in Fas-mediated apoptosis.

Neutrophils purified from human blood express large amounts of gelsolin and undergo spontaneous apoptosis. The rate of neutrophil apoptosis can be further enhanced by cross-linking of Fas or treatment with tumor necrosis factor α (TNFα) and cycloheximide

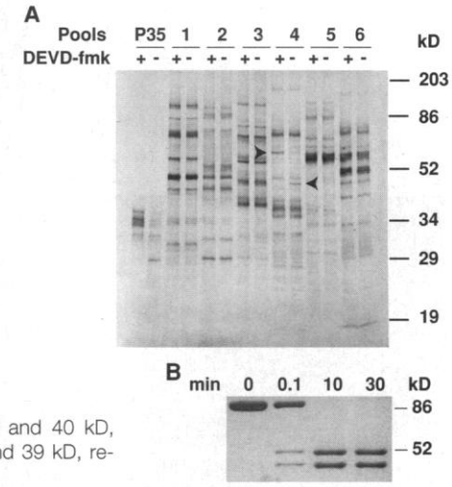

Fig. 1. Identification of gelsolin as a substrate of caspase-3. (**A**) Autoradiogram of [^{35}S]methionine-labeled proteins treated with purified active (–) or inactivated [by addition of a caspase-3 inhibitor, DEVD-fmk (+)] recombinant caspase-3. Lanes 1 through 6 contain the translated proteins from six different representative pools of cDNAs (*23*). The arrows indicate a caspase-3–sensitive protein that is cleaved from an apparent size of 65 kD to 48 kD. This protein was identified as gelsolin. (**B**) Cleavage of bacterially expressed murine gelsolin (*16*) by caspase-3. Gelsolin (13.5 μg) and caspase-3 (6 ng/ml) were incubated at 37°C for the indicated times in 6 mM tris-HCl (pH 7.5), 1.2 mM $CaCl_2$, 5 mM dithiothreitol (DTT), 1.5 mM $MgCl_2$, and 1 mM KCl in a 25 μl volume. A volume of 2 μl was resolved on a gel and stained with Coomassie blue. Bands of apparent size of 48 and 40 kD, corresponding to actual molecular sizes of 41 and 39 kD, respectively, are seen.

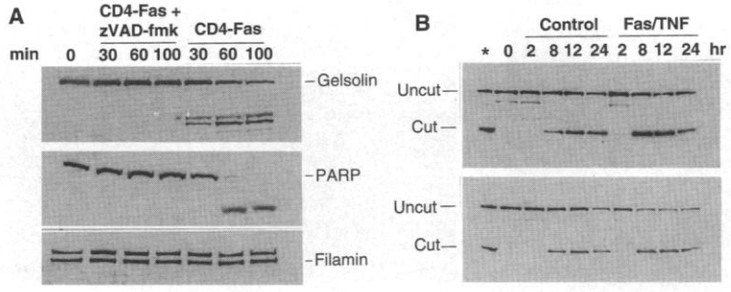

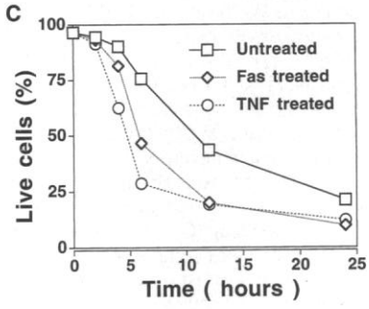

Fig. 2. Gelsolin was cleaved in apoptosis induced by Fas and TNFα. (**A**) Apoptosis was induced by receptor cross-linking with and without 200 μM zVAD-fmk (caspase inhibitor) in murine L929 cells as described (*9*). The cell lysates from an equal number of cells were analyzed by SDS-PAGE and immunoblotted with anti-gelsolin [top panel; polyclonal antibody (*16*)], anti-PARP (middle panel; Enzyme Systems Products), and anti-filamin (bottom; Sigma). The immunoblots were visualized by ECL (Amersham). (**B**) Human neutrophils were isolated with the neutrophil isolation medium (Cardinal Associates) and resuspended in RPMI with 10% fetal bovine serum (FBS) (*24*). Equal numbers of cells were used to prepare cell lysates after incubation with FAS antibody (1 μg/ml, top) or 10 μg/ml TNF and 10 ng/ml cycloheximide (bottom). The lysates were separated by SDS-PAGE and analyzed by immunoblotting with a monoclonal antibody to gelsolin (Sigma), which detects only the COOH-terminal 41-kD fragment. (**C**) Human neutrophils were stained at different time points after isolation from blood, using annexin V apoptosis kit (Clontech), and the number of live cells was estimated by counting the number of annexin- and propidium iodide–negative cells (*24*).

(*11*). To determine if gelsolin is also cleaved when neutrophils undergo apoptosis, we analyzed neutrophil lysates with a monoclonal antibody to gelsolin that recognizes an epitope in the COOH-terminal half of gelsolin. During spontaneous apoptosis in neutrophils, gelsolin amounts decreased and a 41-kD fragment appeared with time (Fig. 2B)—a size identical to fragments generated by cleavage of gelsolin by caspase-3. Increasing the rate of neutrophil apoptosis by cross-linking Fas with antibodies or treatment with TNFα and cycloheximide resulted in an increase in the rate of gelsolin cleavage and appearance of the 41-kD fragment (Fig. 2, B and C). Thus, the cleavage of gelsolin observed in vitro also occurred during apoptosis of neutrophils.

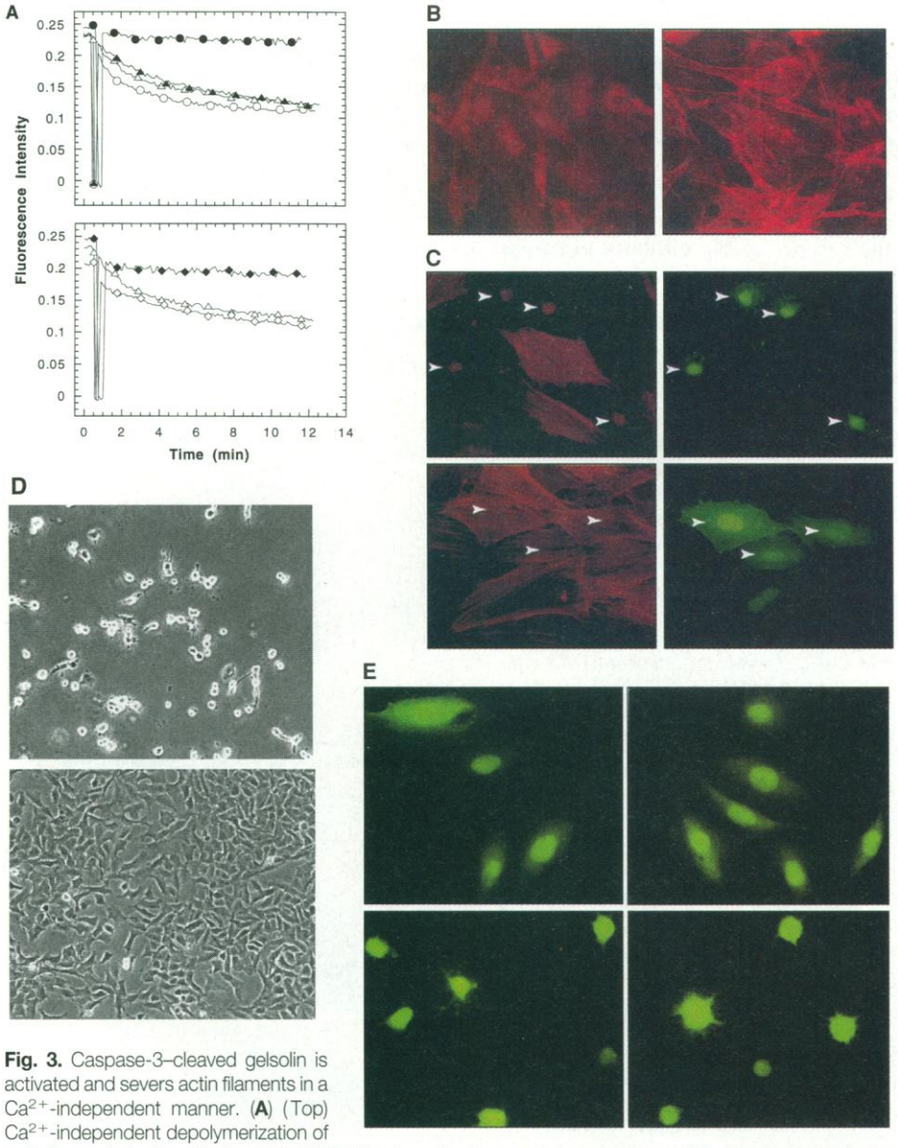

Fig. 3. Caspase-3–cleaved gelsolin is activated and severs actin filaments in a Ca^{2+}-independent manner. (**A**) (Top) Ca^{2+}-independent depolymerization of actin filaments in vitro. We incubated 0.5 μM polymerized pyrene-labeled actin and 50 nM gelsolin (circles) or caspase-3–cleaved gelsolin (triangles) in 2 mM tris-HCl (pH 7.5), 0.5 mM adenosine triphosphate, 0.2 mM DTT, 2 mM $MgCl_2$, and 150 mM KCl, with $CaCl_2$ (0.2 mM; open circles and triangles) or with EGTA (1 mM; solid circles and triangles). The change in pyrene fluorescence with time is shown. (Bottom) Cleaved gelsolin severs F-actin faster than a complex with G-actin is formed. Cleaved gelsolin (20 nM final concentration) was directly added to 0.5 mM F-actin (triangles), or mixed with a twofold molar ratio of G-actin and immediately added (open diamonds) or incubated for 10 min (closed diamonds) and then added to 300 μl of 0.5 μM F-actin. (**B**) Cleaved gelsolin severs the actin cytoskeleton. Permeabilized embryonic fibroblasts ($Gsn^{-/-}$) were incubated with gelsolin or cleaved gelsolin and the actin filaments were visualized by staining with TRITC-phalloidin, as described (*25*). (**C**) The NH_2-terminal gelsolin cleavage fragment induces breakdown of the cytoskeleton. The cells were injected with DNA encoding the NH_2-terminal (top) or COOH-terminal (bottom) fragments of gelsolin and with a plasmid encoding GFP, and were stained for actin filaments with TRITC-phalloidin 5 hours later. The arrows point to the injected cells. The right panel indicates GFP expression, and the left panel indicates actin staining (TRITC-phalloidin) of the same field (*26*). (**D**) Adenovirus expressing the NH_2-terminal gelsolin fragment induces apoptosis. A7 cells (a human melanoma cell line) were infected with adenovirus, prepared as described (*27*), expressing the NH_2-terminal caspase-3 cleavage fragment of gelsolin (residues 1 through 352, top) or full-length gelsolin (1 through 731, bottom). (**E**) The NH_2-terminal gelsolin cleavage fragment induces changes in cell morphology and acts downstream of caspases. The cells were injected with DNA as in (C) and were incubated with dimethyl sulfoxide (left panels) or 100 μM zVAD-fmk (right panels). The injected cells appear green because of GFP expression.

To determine the functional significance of gelsolin cleavage, we examined the activities of cleaved and native gelsolin, using pyrene-actin fluorimetry. In this assay, the conversion of filamentous (F) actin to monomeric (G) actin is monitored by the 25-fold difference in fluorescence between the two states. Native gelsolin severs actin polymers in a Ca^{2+}-dependent manner (*12*, *13*), whereas caspase-3–cleaved gelsolin severed actin polymers independent of Ca^{2+} (Fig. 3A, top). Gelsolin has both actin monomer–binding and F-actin–severing activities (*12*, *13*). However, the cleaved gelsolin preferentially severed actin filaments even when briefly incubated with excess monomeric actin (Fig. 3A, bottom), suggesting that the cleaved gelsolin generated in cells during apoptosis may preferentially sever actin filaments rather than bind monomeric actin. Next, we used permeabilized fibroblasts to determine the ability of cleaved gelsolin to depolymerize the cytoskeletal actin filaments. Cleaved gelsolin depolymerized the actin cytoskeleton in a Ca^{2+}-independent manner, whereas uncut gelsolin was inactive in the presence of EGTA (Fig. 3B).

The actin-severing activity of gelsolin resides in the NH_2-terminal region, residues 1 to 160 (*12*). To test if the NH_2-terminal fragment of gelsolin generated by caspase-3 cleavage could depolymerize actin in vivo, we microinjected DNA encoding the NH_2-terminal fragment (1 to 352) or the COOH-terminal fragment (353 to 731) into fibroblasts. Expression of the NH_2-terminal fragment caused a rapid depolymerization of the actin cytoskeleton, whereas the COOH-terminal fragment had no effect on actin filaments (Fig. 3C). The injection of full-length gelsolin also had no effect on the cell morphology. To determine if gelsolin acts directly to depolymerize actin filaments or indirectly by activating caspases, we incubated the microinjected cells with a caspase inhibitor, zVAD-fmk. Inhibition of caspases did not block the changes in cell morphology induced by the expression of the NH_2-terminal fragment of gelsolin (Fig. 3E). We also constructed adenoviral vectors expressing the NH_2-terminal fragment (1 to 352) or full-

length gelsolin. The adenovirus vector expressing the NH_2-terminal fragment caused rapid cell death in A7 melanoma cells, with both morphologic changes and nuclear fragmentation in the majority of cells within 48 hours of application [determined by terminal deoxytransferase (TdT)–mediated deoxyuridine triphosphate (dUTP) nick-end labeling (TUNEL) staining (*14*)], whereas the full-length construct had no effect (Fig. 3D). A similar result was observed in other cell types, including M2 melanoma cells and NIH 3T3 cells. Both $p53^{+/+}$ and $p53^{-/-}$ murine embryo fibroblasts (*15*) also displayed morphologic changes of apoptosis within 48 hours of infection by the gelsolin NH_2-terminal fragment-expressing adenovirus. Thus, cleavage of gelsolin generated an NH_2-terminal fragment that depolymerizes the actin cytoskeleton in a Ca^{2+}-independent manner, induces cell death, and may be a downstream effector of the morphological changes that are observed during apoptosis.

We used gelsolin null cells derived from $Gsn^{-/-}$ mice (*16*) to examine the importance of gelsolin in apoptosis occurring during physiological stimuli. The course of apoptosis in peritoneal neutrophils treated with TNF plus cycloheximide (TNF+CHX) was assessed by videomicroscopy. Wild-type neutrophils developed blebs as early as 48 min after TNF+CHX, and 52% of cells (32 of 61) had begun blebbing by 6 hours (Fig. 4A). In contrast (Fig. 4B), $Gsn^{-/-}$ neutrophils did not develop blebs until 2 hours 2 min after TNF+CHX, and at 6 hours, only 12% of cells (10 of 83, $P < 0.001$) had blebs. This delay in the progression of apoptosis appeared to contribute directly to a delay in DNA fragmentation in $Gsn^{-/-}$ cells compared with wild-type cells, as assessed in TUNEL assays (Fig. 4C) and DNA analysis by electrophoresis (*17*). No difference in caspase-3 activation was observed when $Gsn^{-/-}$ and wild-type neutrophils were compared, as assessed with the peptide substrate DEVD–7-amino-4-trifluoromethylcoumarin (DEVD-AFC) (*18*), suggesting that the differences seen were from a defect in apoptotic progression downstream of caspase-3 activation. Similar differences in apoptotic progression were seen in $Gsn^{-/-}$ neutrophils in response to treatment with a monoclonal antibody to Fas. Our results may explain the previously observed moderate neutrophilia of $Gsn^{-/-}$ mice, which have approximately twice the number of circulating neutrophils as wild-type mice (*16*).

To confirm the role of cleavage of gelsolin in the morphologic changes of apoptosis, we used the human malignant cell line HeLa, which does not express gelsolin and is relatively resistant to apoptosis (*19*). Gelsolin-expressing, stably transfected HeLa cell lines were more sensitive to human TNFα than were HeLa sublines transfected with control vector alone. Some 72%, 52%, and 38% of the cells from three different gelsolin-expressing HeLa sublines displayed cell rounding and blebbing after treatment with TNF+CHX for 12 hours, while only 8% of the cells from a control line showed these changes.

Caspase or caspase-like cleavage of multiple proteins has been described (*3*, *20*), but few of these are known to have direct physiological significance in the morphologic changes and nuclear degradation that are hallmarks of apoptosis. Using an unbiased approach, we found that the actin-modulating protein gelsolin is the most prominent direct substrate of caspase-3 in murine embryos. Our data also indicate that gelsolin is a probable in vivo target of the apoptotic caspase-initiated cascade and that the gelsolin fragment mediates, in part, the morphologic changes of apoptosis. Blockade or enhancement of gelsolin cleavage might retard or enhance apoptosis in multiple cell types. Gelsolin is the founding member of an evolutionarily conserved family of proteins that extends to *Dictyostelium* and *Drosophila*, and in humans consists of at least six proteins, whose expression is tissue-specific (*21*). Apoptotic cleavage of other gelsolin family members may also occur, and it is possible that these gelsolin homologs have similar roles in mediating apoptotic cytoskeletal changes in specific cell types and tissues. Gelsolin itself is widely expressed in adult mammalian tissues (*13*, *16*), and its expression is specifically down-regulated in many human neoplastic lesions, including bladder, breast, and colon cancer (*22*). These observations on the role of gelsolin in apoptosis suggest that gelsolin down-regulation in tumors may be one mechanism by which tumors evade apoptotic signaling pathways.

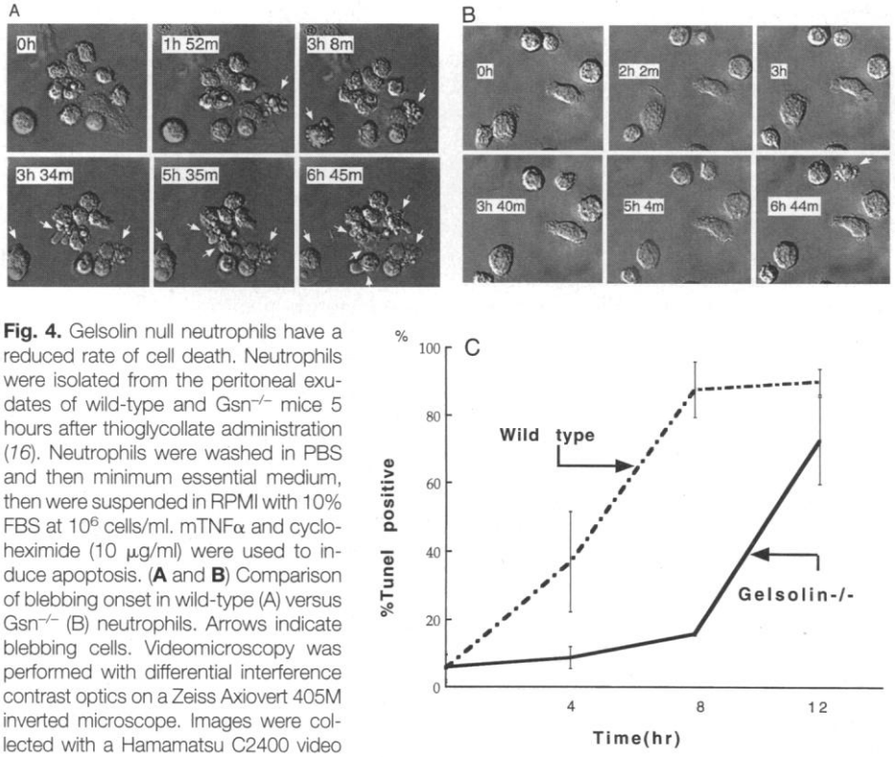

Fig. 4. Gelsolin null neutrophils have a reduced rate of cell death. Neutrophils were isolated from the peritoneal exudates of wild-type and $Gsn^{-/-}$ mice 5 hours after thioglycollate administration (*16*). Neutrophils were washed in PBS and then minimum essential medium, then were suspended in RPMI with 10% FBS at 10^6 cells/ml. mTNFα and cycloheximide (10 μg/ml) were used to induce apoptosis. (**A** and **B**) Comparison of blebbing onset in wild-type (A) versus $Gsn^{-/-}$ (B) neutrophils. Arrows indicate blebbing cells. Videomicroscopy was performed with differential interference contrast optics on a Zeiss Axiovert 405M inverted microscope. Images were collected with a Hamamatsu C2400 video camera (Photonic Microscopy, Bridgewater, New Jersey) and recorded on a Panasonic TQ-3038F video recorder. (**C**) Comparison of DNA fragmentation in $Gsn^{-/-}$ and wild-type neutrophils. The fraction of apoptotic cells as determined by FACS analysis in a TUNEL assay are shown (*14*). $n = 3$ with error bars.

REFERENCES AND NOTES

1. T. Fernandes-Alnemri, G. Litwack, E. S. Alnemri, *J. Biol. Chem.* **269**, 30761 (1994); M. Tewari *et al.*, *Cell* **81**, 801 (1995); K. Kuida *et al.*, *Nature* **384**, 368 (1996); E. S. Alnemri *et al.*, *Cell* **87**, 171 (1996); R. E. Ellis, J. Y. Yuan, H. R. Horvitz, *Annu. Rev. Cell Biol.* **7**, 663 (1991); D. Xue, S. Shaham, H. R. Horvitz, *Genes Dev.* **10**, 1073 (1996).
2. D. W. Nicholson *et al.*, *Nature* **376**, 37 (1995).
3. A. Fraser and G. Evan, *Cell* **85**, 781 (1996).
4. R. W. King, K. D. Lustig, P. T. Stukenberg, T. J. McGarry, M. W. Kirschner, *Science* **277**, 973 (1997); P. T. Stukenberg *et al.*, *Curr. Biol.* **7**, 338 (1997).
5. D. Xue and H. R. Horvitz, *Nature* **377**, 248 (1995).
6. At serial timepoints after induction of apoptosis, extracts were prepared from fibroblasts in 20 mM tris-HCl (pH 7.4), 137 mM NaCl, 1% Triton X-100, and 10% glycerol, and incubated with in vitro synthesized ^{35}S-labeled gelsolin. Cleavage of gelsolin was monitored by SDS-PAGE and autoradiography and occurred concurrently with caspase-3–like activity on DEVD–7-amino-4-methylcoumarin.

7. D. J. Kwiatkowski *et al.*, *Nature* **323**, 455 (1986); M. Way and A. Weeds, *J. Mol. Biol.* **203**, 1127 (1988); C. W. Dieffenbach, D. N. Sen Gupta, D. Krause, D. Sawzak, R. H. Silverman, *J. Biol. Chem.* **264**, 13281 (1989).
8. Native and cleaved gelsolin preparations were analyzed on a BioSil SEC250 column, run in 180 mM NaCl with 10 mM phosphate buffer (pH 7.4) at a flow rate of 1 ml/min, and monitored at 280 nm. Column fractions were analyzed by SDS-PAGE and Coomassie staining.
9. K. Chu, X. Niu, L. T. Williams, *Proc. Natl. Acad. Sci. U.S.A.* **92**, 11894 (1995).
10. E. A. Slee *et al.*, *Biochem. J.* **315**, 21 (1996).
11. W. C. Liles, P. A. Kiener, J. A. Ledbetter, A. Aruffo, S. J. Klebanoff, *J. Exp. Med.* **184**, 429 (1996); Y. Takeda *et al.*, *Int. Immunol.* **5**, 691 (1993).
12. D. J. Kwiatkowski, P. A. Janmey, H. L. Yin, *J. Cell. Biol.* **108**, 1717 (1989).
13. A. G. Weeds, J. Gooch, M. Hawkins, B. Pope, M. Way, *Biochem. Soc. Trans.* **19**, 1016 (1991).
14. Cells (10^6) were fixed with 4% paraformaldehyde and permeabilized with ethanol/acetone. After washing with phosphate-buffered saline (PBS), cells were incubated with TdT and fluorescein-conjugated dUTP at 37°C for 1 hour. Cells were washed, and free DNA ends were visualized by fluorescent microscopy.
15. S. W. Lowe, T. Jacks, D. E. Housman, H. E. Ruley, *Proc. Natl. Acad. Sci. U.S.A.* **91**, 2026 (1994).
16. W. Witke *et al.*, *Cell* **81**, 41 (1995).
17. DNA was prepared from cells by standard digestion and organic extraction. Extracted DNA (10 μg) was separated by electrophoresis in 1.5% agarose and visualized with ethidium staining.
18. Neutrophils (10^5) were treated with TNF+CHX or antibody to Fas, rinsed with PBS, and incubated in 50 mM tris-HCl (pH 7.4), 1 mM EDTA, 10 mM EGTA, and 10 μM digitonin at 37°C for 10 min. After centrifugation at 15,000*g* for 10 min, the lysate was incubated in DEVD-AFC (Enzyme Systems Products) for 30 min. Released AFC was measured by spectrofluorimetry with excitation at a wavelength of 380 nm and emission at 460 nm.
19. R. U. Janicke, X. Y. Lin, F. H. H. Lee, A. G. Porter, *Mol. Cell. Biol.* **16**, 5245 (1996).
20. T. Mashima, M. Naito, N. Fujita, K. Noguchi, T. Tsuruo, *Biochem. Biophys. Res. Commun.* **217**, 1185 (1995); C. Kayalar, T. Ord, M. P. Testa, L. T. Zhong, D. E. Bredesen, *Proc. Natl. Acad. Sci. U.S.A.* **93**, 2234 (1996); Q. Song *et al.*, *ibid.* **94**, 157 (1997); C. Brancolini, M. Benedetti, C. Schneider, *EMBO J.* **14**, 5179 (1995).
21. D. A. Schafer and J. A. Cooper, *Annu. Rev. Cell Dev. Biol.* **11**, 497 (1995); H. D. Campbell *et al.*, *Proc. Natl. Acad. Sci. U.S.A.* **90**, 11386 (1993); D. J. Kwiatkowski *et al.*, unpublished data.
22. M. Tanaka *et al.*, *Cancer Res.* **55**, 3228 (1995); H. L. Asch *et al.*, *ibid.* **56**, 4841 (1996); L. Zhang *et al.*, *Science* **276**, 1268 (1997).
23. A cDNA library was prepared from mouse embryo (day 14 postcoitus) RNA. The cDNAs were cloned into the expression vector pCS2+, generating 200,000 independent clones. The library was fractionated into smaller groups of 100 different clones each. Each group of cDNAs was used to express [^{35}S]methionine-labeled proteins, using a coupled transcription-translation system (TNT system, Promega). We incubated 2 ml of the translation mix with 0.5 ml of active or inactivated caspase-3 (0.15 ng/ml) at 30°C for 0.5 hour. Caspase-3 was inactivated by incubation with 50 mM DEVD-fmk for 30 min before addition to the translation products. Recombinant active caspase-3 was prepared by expressing the sequence of human caspase-3 (YAMA/CPP32, a gift of V. Dixit) in *E. coli* (*2*). Purified caspase-3 (generously provided by A. L. Fear) was fully active when assayed on DEVD–7-amino-4-methylcoumarin as previously described (*3*). Caspase-3 was >80% pure, consisting of 17- and 11-kD subunits, as assayed by SDS-PAGE.
24. S. J. Martin *et al.*, *J. Exp. Med.* **182**, 1545 (1995).
25. A. Huckriede *et al.*, *Cell Motil. Cytoskeleton* **16**, 229 (1990).
26. Rat embryo fibroblasts (REF 52) [T. Joneson, M. A. White, M. H. Wigler, D. Bar-Sagi, *Science* **271**, 810 (1996)] were seeded on acid-treated glass cover slips, and 70% density cells were microinjected with plasmid DNA pGG-NT (encoding residues 1 through 352 of gelsolin and tagged with EYMPME epitope at the COOH-terminus) or pGG-CT (encoding residues 353 through 731 of gelsolin and tagged with EYMPME epitope at the COOH-terminus) at 0.1 μg/ml in 100 mM Hepes (pH 7.4). A plasmid encoding green fluorescent protein (GFP) (pEGFPN1, Promega) at 1 ng/ml was coinjected as a marker. Cells were fixed in 4% paraformaldehyde/PBS, permeabilized with 0.1% Triton X-100, and stained for the expression of tagged proteins, using a mouse monoclonal antibody to EYMPME (50 μg/ml) and a secondary goat anti-mouse immunoglobulin G coupled to Texas Red (Amersham). Actin filaments were visualized with tetramethyl rhodamine isothiocyanate (TRITC)–Phalloidin (Sigma).
27. T. C. Becker *et al.*, *Methods Cell Biol.* **43**, 161 (1994).
28. We thank G. Pronk for p35 cDNA; V. Dixit for YAMA cDNA; A. L. Fear for active caspase-3; A. Creasey and T. Gesner for help with neutrophil isolation; T. Brown, M. Giedlin and T. Shi for fluorescence-activated cell sorter (FACS) analyses; M. Heinzel and G. Harrowe for microscopy; J. Tucker for DNA sequence analyses; and D. A. Fisher and T. Jacks for p53$^{-/-}$ cells. Supported by Chiron Corporation and NIH grants RO1 HL54188 and P01 HL48743 to D.J.K.

9 July 1997; accepted 2 September 1997

V(D)J Recombination in Mature B Cells: A Mechanism for Altering Antibody Responses

Fotini Papavasiliou, Rafael Casellas, Heikyung Suh, Xiao-Feng Qin, Eva Besmer, Roberta Pelanda, David Nemazee, Klaus Rajewsky, Michel C. Nussenzweig*

The clonal selection theory states that B lymphocytes producing high-affinity immunoglobulins are selected from a pool of cells undergoing antibody gene mutation. Somatic hypermutation is a well-documented mechanism for achieving diversification of immune responses in mature B cells. Antibody genes were also found to be modified in such cells in germinal centers by recombination of the variable (V), diversity (D), and joining (J) segments. The ability to alter immunoglobulin expression by V(D)J recombination in the selective environment of the germinal center may be an additional mechanism for inactivation or diversification of immune responses.

One of the key features of adaptive immunity is the ability to respond to an enormous number of different antigens. To account for this diversity the clonal selection theory proposes selective expansion of cells with antibody gene mutations during specific immune responses (*1*). Antibody diversity is initially generated in the bone marrow by a lymphocyte-specific V(D)J recombinase that assembles antigen receptor genes (*2*). Each B cell has only one antibody receptor, a phenomenon known as allelic exclusion (*3*). Exclusion is essential for clonal selection and is established by a feedback mechanism from the membrane-bound B cell receptor (BCR) that extinguishes the expression of the recombinase-activating genes (*RAG1* and *RAG2*) (*4*). Self-reactive BCRs generated during this random gene recombination process can be eliminated in the bone marrow by continued recombination (receptor editing) or by deletion (*5*). B cells leaving the bone marrow are hypothesized to have fixed receptors that can only be altered by somatic hypermutation, a process that would maintain allelic exclusion (*6*). Thus, somatic hypermutation is thought to be the mechanism of antibody gene mutation predicted in the clonal selection theory (*1*).

RAG1 and RAG2 are the recombination signal sequence (RSS)–specific endonucleases that activate V(D)J recombination (*7*). In addition to being found in developing lymphocytes, RAGs are transcribed in germinal centers (*8*), which are the foci of hypermutation (*9*), switch recombination (*10*), and B cell clonal expansion in response to antigen (*11*). The finding that RAGs are expressed in germinal centers suggested that they might mediate antigen receptor diversification in mature B cells that are responding to antigenic stimulation. However, expression of the RAG genes does not necessarily translate into immune receptor gene recombination: *RAG1* is transcribed in the brain, with no known function to date (*12*), and *RAG1*

F. Papavasiliou, R. Casellas, X.-F. Qin, Laboratory of Molecular Immunology, Rockefeller University, New York, NY 10021, USA.
H. Suh, E. Besmer, M. C. Nussenzweig, Laboratory of Molecular Immunology and Howard Hughes Medical Institute, Rockefeller University, New York, NY 10021, USA.
R. Pelanda, Max Plank Institute for Immunobiology, Freiburg, Germany 79108.
D. Nemazee, Division of Basic Sciences, Department of Pediatrics, National Jewish Center for Immunology and Respiratory Medicine, Denver, CO 80206, USA.
K. Rajewsky, Institute for Genetics, University of Cologne, Weyertal, Germany 50931.

*To whom correspondence should be addressed. E-mail: nussen@rockvax.rockefeller.edu